Synthesis of Biomass-based Adsorbent from Rice Husk Ash for Copper Ions Adsorption

Wenlong Liu,[a,b] Xingwen Zhang,[b,]* Hongyu Ren,[c,]* Xingcheng Hu,[b] Xinyu Yang,[b] and Hui Liu [a,]*

To solve the problems of low utilization of agricultural waste rice husk and heavy metal pollution, this investigation prepared a cheap copper ion adsorbent using rice husk ash (RA). The maximum Cu^{2+} adsorption capacity was 19.8 mg/g. X-ray photoelectron spectroscopy (XPS), Fourier transform infrared spectroscopy (FTIR), and surface area and porosity analyses were used to characterize the composition and structure of the material of silica-depleted rice husk ash (SDRA). The thermodynamics and kinetics of Cu^{2+} adsorption by SDRA were studied for their relevance to the adsorption mechanism. The adsorption of copper ions by SDRA was in accordance with the Langmuir model and the pseudo-second-order kinetic model. Furthermore, the increases in specific surface area and oxygen-containing functional groups following silica removal were primarily responsible for SDRA's enhanced adsorption ability. And this is the first time that Cu^{2+} adsorbent has been prepared from the by-product of the synthesis of silane from rice husk ash. So, its synthesis cost is very low. Moreover, the preparation technique of SDRA is a revolutionary method of adsorbent creation that is both economical and environmentally benign.

DOI: 10.15376/biores.18.2.3681-3693

Keywords: Biomass; Ash; Circular economy; Agricultural wastes; Wastewater treatment

Contact information: a: School of Energy Science and Engineering, Harbin Institute of Technology, No. 92, West Dazhi Street, Harbin 150001, China; b: School of Chemistry and Chemical Engineering, Harbin Institute of Technology, No. 92, West Dazhi Street, Harbin 150001, China; c: College of Resources and Environment, Northeast Agriculture University, No. 600, Changjiang Street, Harbin 150001, China;
** Corresponding authors: zhangxingwen@hit.edu.cn; renhongyu@163.com; liuhui@hit.edu.cn*

INTRODUCTION

Rice husk is the major by-product of paddy processing, accounting for about 20% of the paddy grain by weight (Hossain *et al*. 2018). Worldwide, more than 700 million tons of rice are produced annually, and more than 100 million tons of rice husk are generated (Ohta *et al*. 2022). Rice husk is usually agricultural waste, which is discarded directly or burned in the field. These practices take up land resources and release harmful substances, causing environmental pollution (Koul *et al*. 2022). Moreover, it wastes biomass resources. If these rice husks are developed and utilized rationally, they can solve the problem of environmental pollution and improve the profits of farmers. Water pollution is a serious environmental problem, especially for copper; due to its huge demand, a large number of copper products are processed and produced. This leads to a large amount of copper-containing sewage entering rivers and lakes (Karabulut *et al*. 2000; Shabbir *et al*. 2020; Yang *et al*. 2021). When excessive copper ions are absorbed by plants, they interfere with photosynthesis, resulting in reduced crop yields (Shabbir *et al*. 2020). When the body consumes excessive amounts of copper ions, copper affects hematopoietic function, the activity of some enzymes, and the stability of the endocrine system (Gaetke *et al*. 2014). Long-term consumption of drinking water with excessive copper ion content can cause neurological diseases such as depression and Alzheimer's disease (Strausak *et al*. 2001; Zatta *et al*. 2008; Squitti *et al*. 2009). Copper accumulation in the body causes liver cirrhosis and other serious digestive system diseases (Uauy *et al*. 2008). Copper pollution poses a great threat to the health of animals, plants, and humans. Thus, copper pollution control is of great importance.

Currently available methods for treating heavy metals in wastewater include chemical precipitation, electrolysis, reverse osmosis, and membrane separation (Fu *et al*. 2011; Agarwal and Singh 2017). However, the chemical precipitation method produces a large amount of sludge containing heavy metal ions, which can cause secondary pollution. Electrolysis requires a large investment in plant construction and equipment. Reverse osmosis and membrane separation methods are cumbersome and have high operating costs. Compared with other methods, adsorption is a heavy metal ion treatment method with a small investment and simple operation. However, the adsorption effect is influenced by the type of adsorbent. Heavy metal adsorbents include polymers, modified inorganic materials, montmorillonite, activated carbon, and zeolite molecular sieve (Krstić *et al*. 2018; Arora 2019; Vidu *et al*. 2020). However, these adsorbents often suffer from high production costs, environmental pollution during production, complex processes, and poor removal effects. Therefore, it is important to develop low-cost, environmentally friendly, high-performance copper ion adsorbents. Products of incineration and pyrolysis of biomaterials have become a hot research topic in recent years (Das *et al*. 2021a,b,c). Biochar has numerous applications in the field of environmental protection due to its wide source and low cost (Das *et al*. 2022a,b,d). However, no research has been reported on copper ion adsorption using the by-products of silica extraction from rice husk ash. In this study, a high-performance copper ion adsorbent, SDRA, was synthesized from the ash of agricultural waste rice husk. So, the cost is very low. The increases in specific surface area and oxygen-containing functional groups following silica removal were primarily responsible for SDRA’s enhanced adsorption ability. The compositional structures of RA and SDRA were investigated by XPS and FTIR. Then, the effects of factors such as pH, adsorbent dosage, and contact time on the adsorption performance of SDRA were studied. Finally, the adsorption thermodynamics and adsorption kinetics of copper ions adsorption by SDRA were investigated. This is the first time that Cu^{2+} adsorbent has been prepared by the by-product of the synthesis of silane from rice husk ash. This study not only increases the access to rice husk biomass, but also reduces the cost of copper ion adsorbents.

EXPERIMENTAL

Materials

Methanol, hexane, ethanol, and 2-methyl-2,4-pentanediol were purchased from Shanghai Aladdin Biochemical Technology Co., Ltd (Shanghai, China). Rice husk ash was received from the Xing Fu Farm (Qiqihar, China). The process of making rice husk ash was natural incomplete combustion in an ordinary furnace. All reagents were used as received.

Methods

Synthesis of silica-depleted rice husk ash

The SDRA was prepared as reported elsewhere (Laine *et al*. 2016). In brief, a three-necked flask with a capacity of 2 L was used to load 500 g of rice husk ash. 1.2 L of 2-methyl-2,4-pentanediol was added. The mixture was agitated for 30 min, and then the reaction was carried out in an atmosphere of nitrogen at 180 °C with continuous stirring for 48 h. The process of distillation was employed to recover the remaining 2-methyl-2,4-pentanediol as well as spirocyclic alkoxysilane. After distillation, the leftover residue was transferred into a beaker. The residue SDRA was cleaned with methanol, ethanol, and water and oven-dried. Scheme 1 illustrates the synthesis of SDRA from rice husk ash.

Scheme 1. Synthesis of SDRA from rice husk ash

Characterization

The surface area and pore volume of RA and SDRA were analyzed using an ASAP 2020 Plus 1.03 analyzer (Micromeritics Instrument Corp., Norcross, GA, USA). Fourier transform infrared spectroscopy (FTIR, NICOLET IS50, Waltham, MA, USA) was applied to detect the oxygen-containing functional groups of RA and SDRA by the KBr squash method. The elemental composition and surface functional groups of RA and SDRA were measured by X-ray photoelectron spectroscopy (XPS, ESCALAB 250Xi, Thermo Fisher Scientific, Waltham, MA, USA). The concentration of heavy metal ions was detected by ICP-OES (iCAP7400, Thermo Fisher Scientific).

Adsorption experiments

Experiments on the adsorption kinetics of Cu^{2+} by SDRA were carried out for a variety of lengths of time, including 5, 10, 15, 30, 60, 120, 180, 360, 540, 720, 900, 1080, 1260, and 1440 min, at 25 °C and 200 revolutions per min. A sequence of adsorption thermodynamics experiments was carried out at the temperature of 25 °C with an adsorbent mass of 0.1 g, a rotating speed of 200 revolutions per min (rpm), and solutions containing

10, 30, 70, 120, 180, and 270 mg/L of Cu^{2+}, respectively. To study the effect of SDRA dosage on the removal efficiency of Cu^{2+}, 1, 1.5, 2, 2.5, and 3 g/L were used as the dosages of adsorbent to perform adsorption experiments separately. To investigate the influence of pH on Cu^{2+} removal efficiency by SDRA, the adsorption experiments were conducted at pH values of 2, 3, 4, 5, and 6. The removal efficiency of Cu^{2+} by SDRA was computed by Eq. 1. The adsorption capacity of SDRA was computed by Eq. 2.

$$R = \frac{(C_0 - C_e)}{C_0} \times 100\% \tag{1}$$

$$q = \frac{(C_0 - C_e)}{m} \times V \tag{2}$$

where C_0 is the initial copper ions concentration (mg/L), C_e is the equilibrium concentration of copper ions (mg/L), V is the copper ions solution volume (L), and m is the mass of adsorbent in the copper ions solution (g).

RESULTS AND DISCUSSION

Characterization of Ash

BET surface area and pore size analysis

The specific surface area and pore size distribution of SDRA and RA were determined by nitrogen adsorption and desorption experiments. Figure 1 (a) represents the N_2 adsorption-desorption isotherm curves of SDRA and RA. The adsorption isotherms of both SDRA and RA were classified as type IV isotherms according to the IUPAC classification. When the relative pressure P/P_0 is low (0 to 0.5), the adsorption amount increases slowly, and at this time the nitrogen molecules are adsorbed on the inner surface of the rice husk ash from monolayer to multilayer. When the relative pressure P/P_0 is in the interval of 0.5 to 1, the adsorption amount rises significantly, and the adsorption and desorption curves appear to be separated from each other. The desorption isotherm was observed to be above the adsorption isotherm. Thus, it belonged to the H3 adsorption hysteresis loop judged according to the criteria of the hysteresis loop in IUPAC. This indicates the presence of a mesoporous structure in rice husk ash.

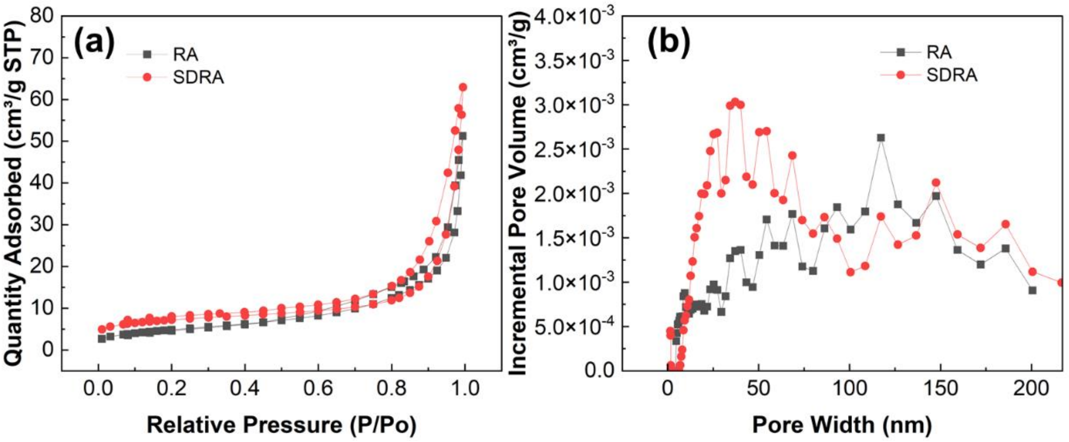

Fig. 1. (a) nitrogen adsorption-desorption isotherms of RA and SDRA (b) pore diameter distribution of RA and SDRA

According to the pore size distribution graphs of RA and SDRA (Fig. 1 (b)), the number of mesopores in SDRA increased significantly in the size range of 0 to 50 nm compared with RA, and the mesopores were mainly concentrated around 35 nm, which is consistent with the results of the adsorption-desorption isotherm curve of SDRA.

The specific surface area and pore structure parameters of RA and SDRA are shown in Table 1. Compared with RA, the specific surface area of SDRA increased from 17.7 to 26.0 m^2g^{-1}, an increase of 47.0%. The pore volume was increased from 0.0793 to 0.0941 cm^3g^{-1}, an increase of 18.7%.

Table 1. Specific Surface Area and Pore Structure of RA and SDRA

	BET Specific Surface Area (m^2 g^{-1})	Specific Pore Volume (cm^3 g^{-1})
RA	17.7	0.0793
SDRA	26.0	0.0941

XPS analysis

To analyze the chemical environment of the elements on the material surface, XPS tests were performed for RA and SDRA, respectively. The results are shown in Fig. 2. The full spectra of RA and SDRA are shown in Fig. 2(a) and Fig. 2(b), respectively. The results show that they both exhibited peaks near 103.6 eV, 284.6 eV, and 532.8 eV, and these peaks can be attributed to Si2p, C1s, and O1s, respectively.

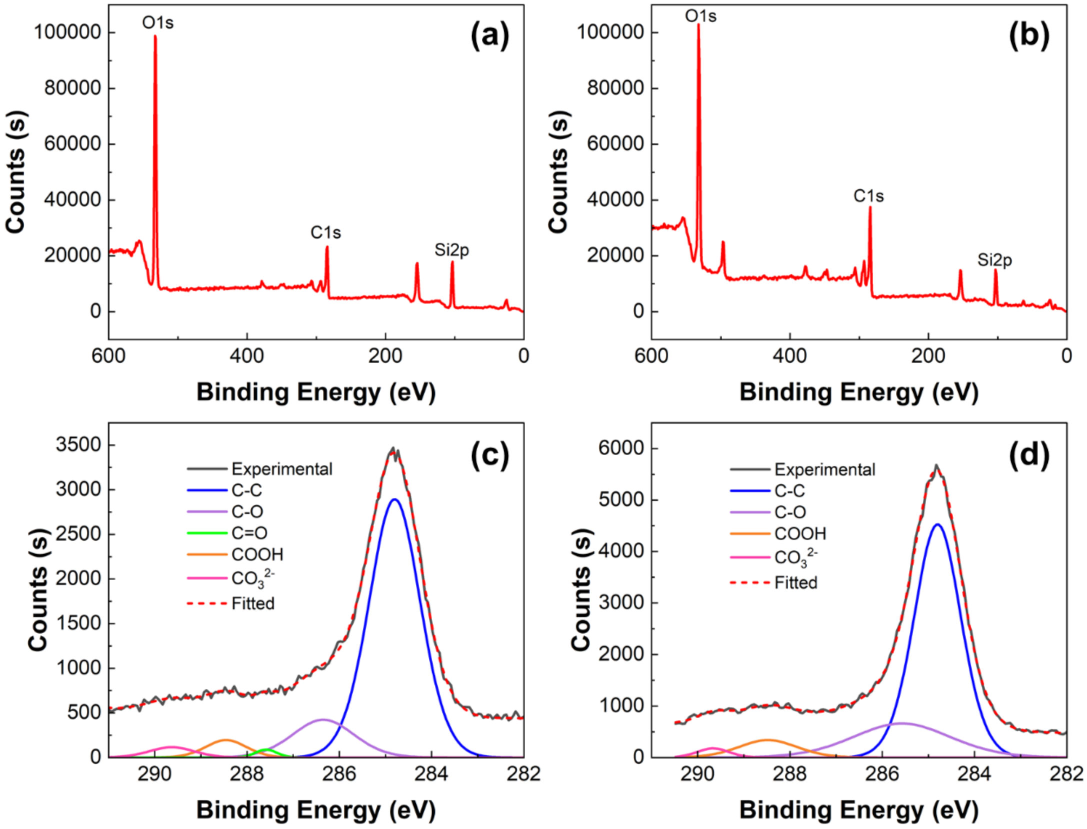

Fig. 2. XPS spectra (a) wide survey of RA (b) wide survey of SDRA (c) high-resolution C1s of RA (d) high-resolution C1s of SDRA

The C1s of RA and SDRA were analyzed at high resolution. The spectra are shown in Fig. 2(c) and Fig. 2(d). The result showed that the C1s of SDRA were divided into four peaks located near 284.8 eV, 285.58 eV, 288.48 eV, and 289.67 eV, which were attributed to C-C, C-O, COOH, and CO_3^{2-}, respectively. The contents of C-O and COOH in SDRA increased significantly from 13.8% and 4.23% to 21.33% and 6.57%, respectively, compared with those in RA. As a result, there was a significant increase in the content of oxygen-containing functional groups in SDRA, which is consistent with the results of FTIR analysis.

FTIR analysis

FTIR was used to analyze the functional groups of rice husk ash after silica removal. Figure 3 displays the FTIR results. The absorbance peak at 2940 cm^{-1} was generated by the stretching vibration of -OH in the carboxyl group. The peak at 3380 cm^{-1} was generated by the stretching vibration of -OH. The peak at 1580 cm^{-1} was generated by the stretching vibration of C=O in the aromatic conjugated ketones and quinones. The peak at 1050 cm^{-1} was generated by the stretching vibration of C-O. The RA and SDRA absorbance peaks appeared at approximately the same position. Compared with RA, the peak area and absorption intensity of the peak at the above position of SDRA were significantly increased. This indicates that the contents of -COOH, -OH, C=O and C-O in SDRA were significantly elevated. These oxygen-containing functional groups can act as active sites for the adsorption of copper ions during the adsorption process.

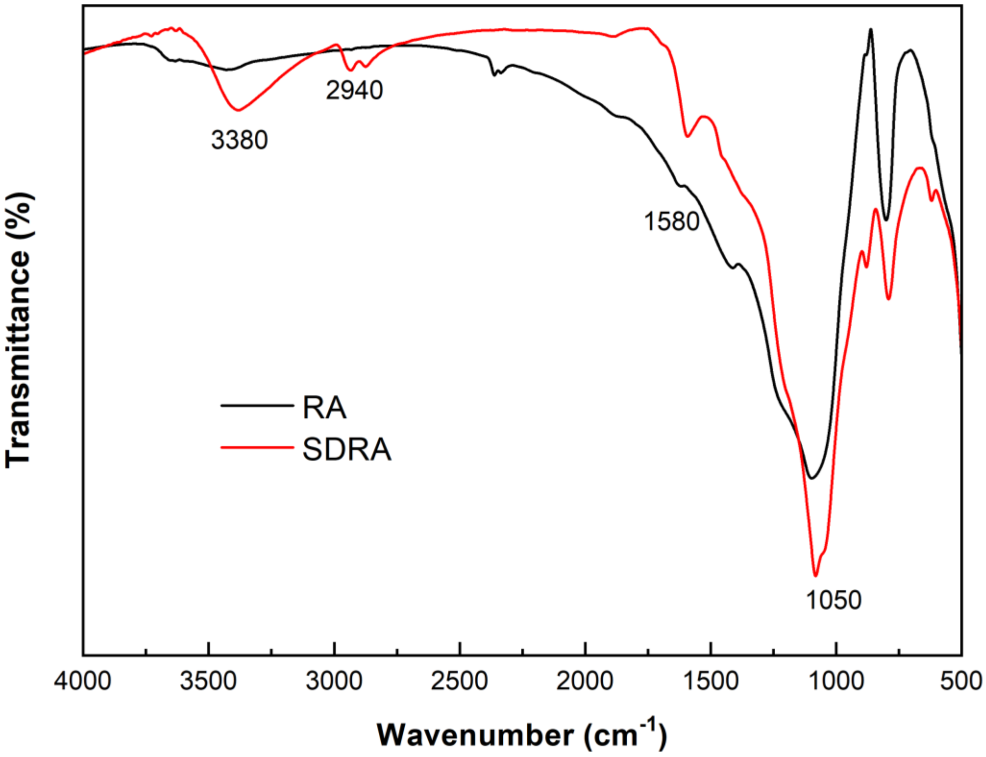

Fig. 3. Infrared spectra of RA and SDRA

Adsorption Experiments

Effect of adsorbent dosage and pH

The effect of SDRA mass concentration on the removal efficiency of Cu^{2+} is shown in Fig. 4(a). With the increasing mass concentration of SDRA, its removal efficiency of Cu^{2+} also increased, and the increasing trend was fast at first and then slow. When the mass concentration of SDRA was 1 g/L, the removal efficiency of Cu^{2+} by SDRA was 56.0%. When the mass concentration of SDRA was 3 g/L, the removal efficiency of Cu^{2+} by SDRA was 98.87%. When the mass concentration of SDRA was 2.5 g/L, the adsorption capacity of SDRA on Cu^{2+} tended to be stable, and the removal efficiency of SDRA on Cu^{2+} was 98.09%. Therefore, the optimal test condition was the SDRA mass concentration of 2.5 g/L.

In addition, the adsorption experiments of SDRA on Cu^{2+} under different acidic conditions were carried out in this study. The effect of SDRA on the removal efficiency of Cu^{2+} under different acidic conditions is shown in Fig. 4(b).

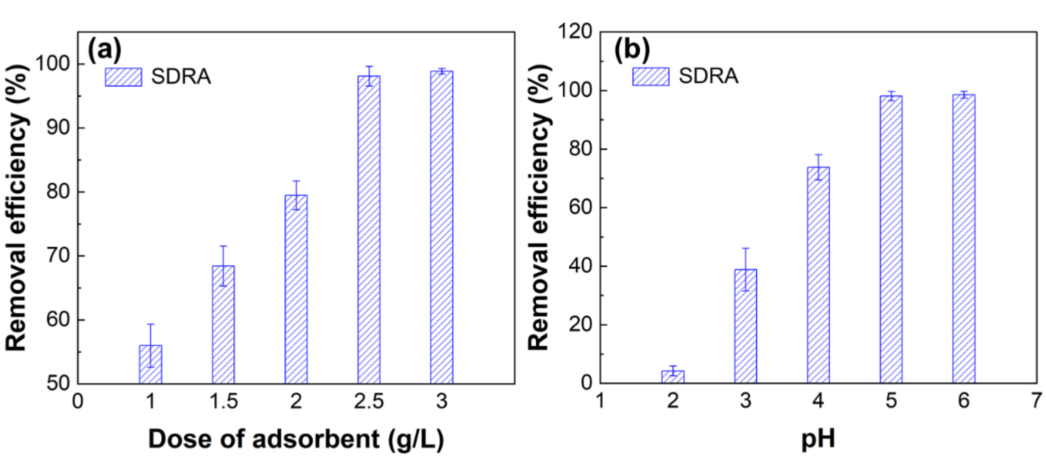

Fig. 4. Effect of dose of SDRA (a) and pH (b) on Cu removal

The removal efficiency of Cu^{2+} by SDRA increased with the increase of pH, from 4.21% at pH 2 to 98.6% at pH 6. The reason is that pH not only affects the protonation degree of active groups on the surface of SDRA, but also affects the ionic distribution of Cu^{2+} in aqueous solution. Low pH causes the change of electrostatic repulsion between protonated groups and Cu^{2+} in solution. H_3O^+ forms a competitive adsorption relationship with positively charged Cu^{2+}, which results in the low removal efficiency of Cu^{2+}. By contrast, the increase of pH causes Cu^{2+} to form metal ion hydroxylated complexes, which facilitates the immobilization of Cu^{2+} by SDRA. The amount of Cu^{2+} adsorption increased. The removal efficiency at pH 5 was only 0.46% less than that at pH 6. Therefore, pH 5 was chosen as the test condition for overall consideration.

Adsorption kinetics

The adsorption kinetics mainly investigates the variation of adsorption rate with time, and the kinetic process of Cu^{2+} adsorption by SDRA was fitted by introducing pseudo-first and -second-order kinetic equations, respectively, which are shown as follows,

$$\ln(Q_e - Q_t) = \ln Q_e - k_1 t \tag{3}$$

$$\frac{t}{Q_t} = \frac{1}{k_2 Q_e^2} + \frac{t}{Q_e} \tag{4}$$

where *t* is the adsorption time (min); Q_e is the adsorption amount of Cu^{2+} at equilibrium ($mg \cdot g^{-1}$); Q_t is the adsorption amount of Cu^{2+} at time *t* ($mg \cdot g^{-1}$); k_1 is the adsorption rate constant of pseudo-first-order kinetic equation (min^{-1}); and k_2 is the adsorption rate constant of pseudo-second-order kinetic equation ($g \cdot mg^{-1} \cdot min^{-1}$).

Figure 5 shows the fitted curves of the pseudo-first and -second-order kinetic equations for Cu^{2+} adsorption by SDRA, and the obtained fitted parameters are shown in Table 2.

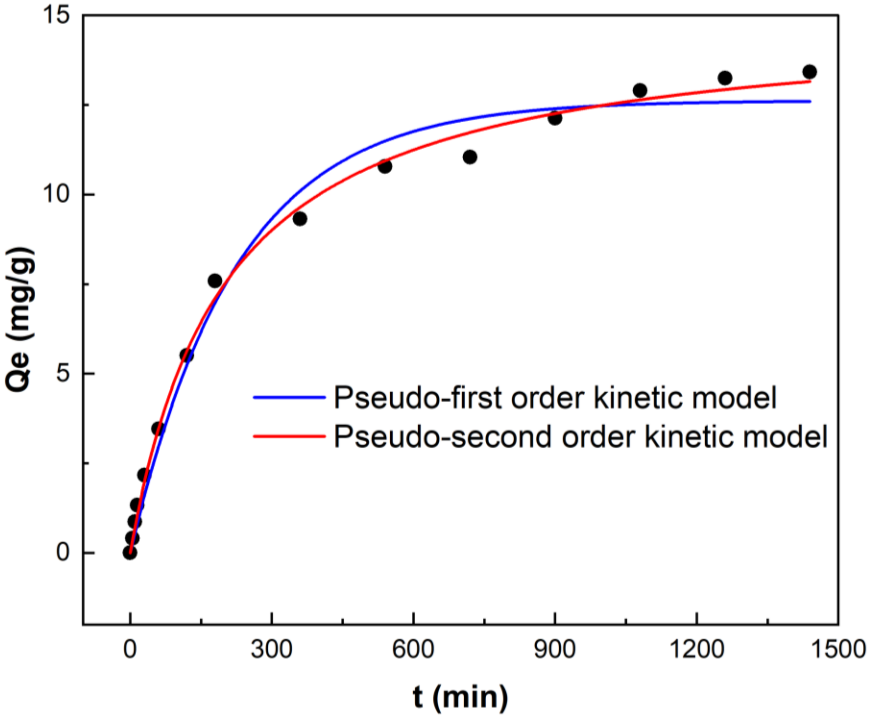

Fig. 5. Pseudo-first and -second-order kinetic model for the adsorption of Cu^{2+} onto SDRA.

Table 2. Pseudo-first and Second-order Kinetic Model Constant

kinetic model	R^2	C_0 (mg/L)	$Q_{e,\,cal}$ (mg/g)	$Q_{e,\,exp}$ (mg/g)
Pseudo-first order kinetic model	0.987	120	12.62	16.40
Pseudo-second order kinetic model	0.997	120	14.97	16.40

Based on the calculated results of the experiment data, the R^2 fitted by the pseudo-first-order kinetic model was 0.987. However, the R^2 fitted by the pseudo-second-order kinetic model was 0.997. The calculated value of equilibrium adsorption $Q_{e,\,cal}$ fitted by the pseudo-first-order kinetic model was 12.62 $mg \cdot g^{-1}$. The calculated value of equilibrium adsorption $Q_{e.cal}$ fitted by the pseudo-second-order kinetic model was 14.97 $mg \cdot g^{-1}$, which was closer to the experimentally determined value of $Q_{e,exp}$ (16.40 $mg \cdot g^{-1}$). These results indicate that the pseudo-second-order kinetic model was a better fit for describing the adsorption of Cu^{2+} by SDRA.

Adsorption isotherms

The adsorption processes of SDRA and RA on Cu^{2+} were described using Freundlich and Langmuir isothermal equations, which are shown as follows,

$$Q_e = \frac{Q_m K_L C_e}{1 + Q_m K_L C_e} \tag{5}$$

$$Q_e = K_F C_e^{1/n} \tag{6}$$

where *t* is adsorption time (min); C_e is concentration of Cu^{2+} at equilibrium ($mg \cdot L^{-1}$); Q_m is maximum adsorption amount of Cu^{2+} ($mg \cdot g^{-1}$); K_L is Langmuir constant ($L \cdot mg^{-1}$); K_f is Freundlich constant ($mg \cdot g^{-1}$); and 1/*n* is Freundlich exponent.

The results are shown in Fig. 6. The experimental data were fitted and calculated, respectively, and the results are shown in Table 3. The Langmuir adsorption isotherm model was able to well describe the thermodynamic processes of Cu^{2+} adsorption by SDRA and RA with R^2 of 0.995 and 0.981 respectively. For SDRA, the Langmuir model fit better than the Freundlich model.

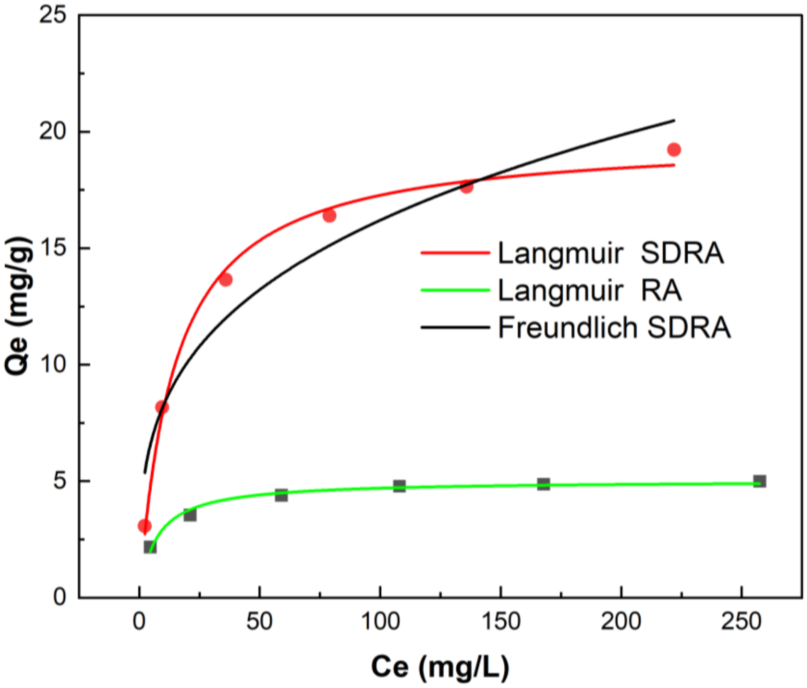

Fig. 6. Adsorption isotherm of RA and SDRA

Table 3. Isotherm Parameters for Cu^{2+} Adsorption by RA and SDRA

Adsorbent	Langmuir model		Freundlich model	
	Q_m (mg/g)	R^2	K_f (mg/g)	R^2
SDRA	19.8	0.995	4.19	0.942
RA	5.03	0.981		

The Langmuir model is derived from a series of assumptions that all of the adsorption sites are assumed to be equal and non-interacting. The maximum adsorption amounts of Cu^{2+} by SDRA and RA derived from Langmuir model were 19.8 mg/g and 5.03 mg/g, respectively. The data in Table 4 shows that SDRA had the highest adsorption capacity among the several biomass adsorbents examined in the previous study. Furthermore, this study was using the by-product of the synthesis of spirocyclosilane (Laine *et al.* 2016), a high-value-added silicon product. The purpose of this reaction is mainly to obtain high-purity silicone, which is an important industrial raw material. Thus, the approach used in the present work will also benefit from financial compensation for helping to dispose of the remaining large amount of residue after extraction of the spirocyclosilane. This is equivalent to turning waste into treasure. The removal of silica results in the formation of more cavernous structures within the rice husk ash, and thus SDRA has a higher specific surface area compared to RA. And the higher specific surface area provides more adsorption sites. More importantly, the content of oxygen-containing functional groups in SDRA was significantly increased after the silica removal treatment. This significantly increased the active sites for adsorption.

Table 4. Maximum Cu(II) Adsorption Capacities of Various Biomass Adsorbents.

Metal	Biomass	Q_m (mg/g))	Reference
Cu(II)	Goethite biochar	5.38	(Guo *et al*. 2016)
Cu(II)	Hard wood	6.79	(Chen *et al*. 2011)
Cu(II)	Acid-treated bio-sorbent	8	(Al Ketife et al. 2021)
Cu(II)	Biochar	8.85	(Adeyemo et al. 2014)
Cu(II)	Banana peel	9.5	(Li *et al*. 2016)
Cu(II)	Willow wood	12.2	(Wang *et al*. 2020)
Cu(II)	Sunflower husks & rapeseed pomace	17.10	(Tomczyk *et al*. 2020)

CONCLUSIONS

1. In this study, for the first time, an adsorbent for copper ions was prepared from the by-product of the synthesis of spirocyclosilane from rice husk ash. This is equivalent to solving another industrial by-product treatment problem. Thus, the cost of this adsorbent is very low.
2. The maximum adsorption capacity of SDRA was 19.8 mg/g. The adsorption of copper ions by SDRA was found to be in accordance with the Langmuir model and the pseudo-second-order kinetic model.
3. There was a significant increase in the specific surface area (compared with RA, the specific surface area of SDRA increased from 17.7 to 26.0 m^2g^{-1}, an increase of 47.0%) and oxygen-containing functional groups (the contents of C-O and COOH in SDRA increased significantly from 13.8% and 4.23% to 21.33% and 6.57%, respectively, compared with those in RA) of SDRA after silica removal was the main mechanism of the improved adsorption performance.
4. This study broadens the utilization of rice husk biomass while solving the problem of the high cost of copper ion adsorbent. In the next work, we will also continue to explore the recovery and reuse methods of adsorbent.

ACKNOWLEDGMENTS

The authors are grateful for the support of the Harbin Institute of Technology.

REFERENCES CITED

Agarwal, M., and Singh, K. (2017). "Heavy metal removal from wastewater using various adsorbents: a review," *Journal of Water Reuse and Desalination* 7(4), 387-419. DOI: 10.2166/wrd.2016.104

Arora, R. (2019). "Adsorption of heavy metals–A review," *Materials Today: Proceedings* 18, 4745-4750. DOI: 10.1016/j.matpr.2019.07.462

Chen, X., Chen, G., Chen, L., Chen, Y., Lehmann, J., McBride, M. B., and Hay, A. G. (2011). "Adsorption of copper and zinc by biochars produced from pyrolysis of hardwood and corn straw in aqueous solution," *Bioresource Technology* 102(19), 8877-8884. DOI: 10.1016/j.biortech.2011.06.078

Das, S. K., and Ghosh, G. K. (2021a). "Developing biochar-based slow-release NPK fertilizer for controlled nutrient release and its impact on soil health and yield," *Biomass Conversion and Biorefinery*. DOI: 10.1007/s13399-021-02069-6

Das, S. K., and Ghosh, G. K. (2021b). "Development and evaluation of biochar-based secondary and micronutrient enriched slow release nano-fertilizer for reduced nutrient losses," *Biomass Conversion and Biorefinery*. DOI: 10.1007/s13399-021-01880-5

Das, S. K., and Ghosh, G. K. (2022a). "Conversion of biomass into low-cost biochar along with organic manure improved soil hydro-physical environment through technological intervention for sandy soil restoration," *Biomass Conversion and Biorefinery*. DOI: 10.1007/s13399-022-02724-6

Das, S. K., and Ghosh, G. K. (2022b). "Soil hydro-physical properties affected by biomass-derived biochar and organic manure: a low-cost technology for managing acidic mountain sandy soils of north eastern region of India," *Biomass Conversion and Biorefinery*. DOI: 10.1007/s13399-022-03107-7

Das, S. K., Ghosh, G. K., and Avasthe, R. (2022c). "Biochar and organic manures on produce quality, energy budgeting, and soil health in maize-black gram system," *Arabian Journal of Geosciences* 15(18), article 1527. DOI: 10.1007/s12517-022-10790-3

Das, S. K., Ghosh, G. K., Choudhury, B., Hazarika, S., and Mishra, V. (2022d). "Developing biochar and organic nutrient packages/technology as soil policy for enhancing yield and nutrient uptake in maize-black gram cropping system to maintain soil health," *Biomass Conversion and Biorefinery*. DOI: 10.1007/s13399-022-02300-y

Fu, F., and Wang, Q. (2011). "Removal of heavy metal ions from wastewaters: A review," *Journal of Environmental Management* 92(3), 407-418. DOI: 10.1016/j.jenvman.2010.11.011

Gaetke, L. M., Chow-Johnson, H. S., and Chow, C. K. (2014). "Copper: Toxicological relevance and mechanisms," *Archives of toxicology* 88(11), 1929-1938. DOI: 10.1007/s00204-014-1355-y

Guo, X., Dong, H., Yang, C., Zhang, Q., Liao, C., Zha, F., and Gao, L. (2016). "Application of goethite modified biochar for tylosin removal from aqueous solution," *Colloids and Surfaces A: Physicochemical and Engineering Aspects* 502, 81-88. DOI: 10.1016/j.colsurfa.2016.05.015

Hossain, S. S., Mathur, L., and Roy, P. (2018). "Rice husk/rice husk ash as an alternative source of silica in ceramics: A review," *Journal of Asian Ceramic Societies* 6(4), 299-313. DOI: 10.1080/21870764.2018.1539210

Karabulut, S., Karabakan, A., Denizli, A., and Yürüm, Y. (2000). "Batch removal of copper (II) and zinc (II) from aqueous solutions with low-rank Turkish coals," *Separation and Purification Technology* 18(3), 177-184. DOI: 10.1016/S1383-5866(99)00067-2

Koul, B., Yakoob, M., and Shah, M. P. (2022). "Agricultural waste management strategies for environmental sustainability," *Environmental Research* 206, article 112285. DOI: 10.1016/j.envres.2021.112285

Krstić, V., Urošević, T., and Pešovski, B. (2018). "A review on adsorbents for treatment of water and wastewaters containing copper ions," *Chemical Engineering Science* 192, 273-287. DOI: 10.1016/j.ces.2018.07.022

Laine, R.M., Furgal, J.C., Doan, P., Pan, D., Popova, V., and Zhang, X. (2016). "Avoiding carbothermal reduction: Distillation of alkoxysilanes from biogenic, green, and sustainable sources," *Angewandte Chemie* 55(3), 1077-1081. DOI: 10.1002/anie.201506838

Li, J., Dai, J., Liu, G., Zhang, H., Gao, Z., Fu, J., He, Y., and Huang, Y. (2016). "Biochar from microwave pyrolysis of biomass: A review," *Biomass and Bioenergy* 94, 228-244. DOI: 10.1016/j.biombioe.2016.09.010

Ohta, S., Yoshida, K., and Hongo, T. (2022). "Synthesis of allophane from rice husk ash and its use as a phosphate adsorbent: A novel approach," *Journal of Environmental Chemical Engineering* 10(6), article 108634. DOI: 10.1016/j.jece.2022.108634

Shabbir, Z., Sardar, A., Shabbir, A., Abbas, G., Shamshad, S., Khalid, S., Murtaza, G., Dumat, C., and Shahid, M. (2020). "Copper uptake, essentiality, toxicity, detoxification and risk assessment in soil-plant environment," *Chemosphere* 259, article 127436. DOI: 10.1016/j.chemosphere.2020.127436

Squitti, R., Bressi, F., Pasqualetti, P., Bonomini, C., Ghidoni, R., Binetti, G., Cassetta, E., Moffa, F., Ventriglia, M., and Vernieri, F. (2009). "Longitudinal prognostic value of serum “free” copper in patients with Alzheimer disease," *Neurology* 72(1), 50-55. DOI: 10.1212/01.wnl.0000338568.28960.3f

Strausak, D., Mercer, J. F., Dieter, H. H., Stremmel, W., and Multhaup, G. (2001). "Copper in disorders with neurological symptoms: Alzheimer’s, Menkes, and Wilson diseases," *Brain Research Bulletin* 55(2), 175-185. DOI: 10.1016/S0361-9230(01)00454-3

Tomczyk, A., Sokołowska, Z., and Boguta, P. (2020). "Biomass type effect on biochar surface characteristic and adsorption capacity relative to silver and copper," *Fuel* 278, article 118168. DOI: 10.1016/j.fuel.2020.118168

Uauy, R., Maass, A., and Araya, M. (2008). "Estimating risk from copper excess in human populations," *The American journal of clinical nutrition* 88(3), 867S-871S. DOI: 10.1093/ajcn/88.3.867S

Vidu, R., Matei, E., Predescu, A.M., Alhalaili, B., Pantilimon, C., Tarcea, C., and Predescu, C. (2020). "Removal of heavy metals from wastewaters: A challenge from current treatment methods to nanotechnology applications," *Toxics* 8(4), 101. DOI: 10.3390/toxics8040101

Wang, S., Kwak, J.-H., Islam, M. S., Naeth, M. A., El-Din, M. G., and Chang, S. X. (2020). "Biochar surface complexation and Ni (II), Cu (II), and Cd (II) adsorption in aqueous solutions depend on feedstock type," *Science of the Total Environment* 712, article 136538. DOI: 10.1016/j.scitotenv.2020.136538

Yang, L., Peng, Y., Qian, C., Xing, G., He, J., Zhao, C., and Lai, B. (2021). "Enhanced adsorption/photocatalytic removal of Cu (II) from wastewater by a novel magnetic chitosan@ bismuth tungstate coated by silver (MCTS-Ag/Bi_2WO_6) composite," *Chemosphere* 263, article 128120. DOI: 10.1016/j.chemosphere.2020.128120

Zatta, P., Drago, D., Zambenedetti, P., Bolognin, S., Nogara, E., Peruffo, A., and Cozzi, B. (2008). "Accumulation of copper and other metal ions, and metallothionein I/II expression in the bovine brain as a function of aging," *Journal of Chemical Neuroanatomy* 36(1), 1-5. DOI: 10.1016/j.jchemneu.2008.02.008

Article submitted: November 12, 2022; Peer review completed: November 30, 2023; Revised version received: March 30, 2023; Further revisions received and article accepted: April 6, 2023; Published: April 13, 2023.
DOI: 10.15376/biores.18.2.3681-3693